SIAM J. SCI. COMPUT.
Vol. 41, No. 1, pp. A643–A667

STABILITY OF ENERGY STABLE FLUX RECONSTRUCTION FOR THE DIFFUSION PROBLEM USING COMPACT NUMERICAL FLUXES*

SAMUEL QUAEGEBEUR†, SIVAKUMARAN NADARAJAH†, FARSHAD NAVAH†, AND PHILIP ZWANENBURG‡

Abstract. Recovering some prominent high-order approaches such as the discontinuous Galerkin or the spectral difference methods, the flux reconstruction framework has been adopted by many individuals in the research community and is now commonly used to solve problems on unstructured grids over complex geometries. This approach relies on the use of correction functions to obtain a differential form for the discrete problem. A class of correction functions, named energy stable flux reconstruction functions, has been proven stable for the linear advection problem. This proof has then been extended to the diffusion equation using the local discontinuous Galerkin (LDG) method to compute the numerical fluxes. Although the LDG formulation is commonly used, many prefer other compact numerical fluxes such as the interior penalty (IP), the Bassi and Rebay II, the compact discontinuous Galerkin, or the compact discontinuous Galerkin 2 numerical fluxes. Similarly to the LDG proof, this article provides a stability analysis for these compact formulation. In fact, we obtain a theoretical condition on the penalty term to ensure stability. This result is then verified through numerical simulations for the IP approach.

Key words. ESFR methods, diffusion, stability, interior penalty numerical fluxes, Bassi and Rebay 2 numerical fluxes, compact discontinuous Galerkin numerical fluxes

AMS subject classification. 65N12

DOI. 10.1137/18M1184916

1. Introduction.

The discontinuous Galerkin (DG) method, proposed by Reed and Hill [20], combines the interesting properties of finite volume and finite element methods. As explained in the book of Hesthaven and Warburton [12], it uses numerical fluxes to provide stability and high-order shape functions to represent the solution. In the last two decades, theoretical and numerical results have contributed to widen the knowledge of the method. Concerning the diffusion equation, many numerical fluxes have been developed such as the interior penalty (IP) [1], the Bassi and Rebay II (BR2) [2], the local discontinuous Galerkin (LDG) [8], the compact discontinuous Galerkin (CDG) [14], and the compact discontinuous Galerkin 2 (CDG2) [3]. All of these methods contain a penalty term, which accounts for the jump between the cells or control volumes. Choosing this parameter appropriately ensures stability.

The unifying framework of flux reconstruction (FR), developed by Huynh [9], [10], enables the recovery, through the use of correction functions, of not only the DG method but also other high-order methods such as spectral difference (SD) [13] and spectral volumes. These methods are of special interest since, as shown in [9] and [10] through a von Neumann analysis, they allow for a larger time step compared to DG;

*Submitted to the journal's Methods and Algorithms for Scientific Computing section May 2, 2018; accepted for publication (in revised form) December 17, 2018; published electronically February 28, 2019.

http://www.siam.org/journals/sisc/41-1/M118491.html

Funding: This work was supported by the Natural Sciences and Engineering Research Council of Canada Discovery Grant Program and by McGill University.

†Mechanical Engineering, McGill University, Montreal, H3A 0C3, PQ, Canada (samuel.quaegebeur@mail.mcgill.ca, siva.nadarajah@mcgill.ca, farshad.navah@mail.mcgill.ca).

‡The author is deceased. Former address: Mechanical Engineering, McGill University, Montreal, H3A 0C3, PQ, Canada.

however few studies have been achieved on their stability. In order to fill this gap of knowledge, Vincent [19] defined a class of correction functions called the Vincent–Castonguay–Jameson–Huynh (VCJH) schemes, containing DG, SD, and g_2, which are stable for the linear advection problem. The mathematical proof is based on the energy of the solution and hence this class has taken the name of energy stable flux reconstruction (ESFR) schemes. This proof was extended to the diffusion equation by Castonguay et al. [7]. Employing the LDG numerical flux and the ESFR correction functions, they proved that taking a positive penalty term ensures the stability of the method. The purpose of this article is to extend the theoretical proof of [7] to the compact IP, BR2, CDG, and CDG2 numerical fluxes. This article is composed as follows. Section 3 shows that the method is independent of the auxiliary correction function when employing the IP or the BR2 numerical flux. Section 4 contains the theoretical proof of stability for the IP scheme and numerical verifications, and section 5 presents the analogy between the IP formulation and the BR2, CDG, and CDG2 numerical fluxes. We conclude this paper with section 6, presenting the L_2-errors for a representative problem. Therefore this article allows us to make a sensible choice of parameters in order to combine a stable scheme with a high time step and a correct order of accuracy (OOA). As the theoretical result is based on the work of Castonguay et al. [7], we strongly advise the reader to consult this reference a priori. The current article will use similar notation in an attempt to be as comprehensible as possible.

2. Preliminaries. We present, briefly, the FR scheme for the diffusion problem and introduce the notation used throughout this article. The FR approach is based on the work of Huynh [10].

Let us consider the diffusion equation,

$$\frac{\partial u}{\partial t} = b\Delta u,\ x \in \Omega,\ t \in [0,T]\,, \tag{2.1}$$

where $u(x,t)$ is the solution in the physical space, b is the diffusion parameter, Δ is the Laplacian operator, Ω is the physical domain, and T is a positive value. We apply the tesselation $\mathcal{T}_h = \sum_{n=1}^{N_K} \Omega_n$ such that the spatial domain Ω is approximated by N_K nonoverlapping and continuous elements where Ω_n is the nth element. The second-order PDE (2.1) can be written as a system of two first-order equations,

$$\frac{\partial u_n}{\partial t} = b\nabla q_n, \tag{2.2a}$$

$$q_n = \nabla u_n, \tag{2.2b}$$

where $\nabla = \frac{\partial}{\partial x}$.

We refer to (2.2a) as the primary equation and (2.2b) as the auxiliary equation. Equations (2.2a) and (2.2b) are valid on each element $\Omega_n = [x_n, x_{n+1}]$, $n \in [\![1, N_K]\!]$ (an interval of the type $[\![.,.]\!]$ denotes an integer interval). We note u_n and q_n the solution and the corrected gradient on the element Ω_n. We then map the equation from the physical into the computational space through the affine mapping $\mathcal{M}_n$,

$$\begin{array}{rccl} \mathcal{M}_n\colon & [-1,1] & \to & \Omega_n, \\ & r & \mapsto & \dfrac{(1-r)}{2}x_n + \dfrac{(1+r)}{2}x_{n+1}. \end{array} \tag{2.3}$$

The Jacobian of this mapping in element Ω_n is noted as J_n,

$$J_n = \frac{\mathrm{d}x}{\mathrm{d}r} = \frac{\mathrm{d}\mathcal{M}_n(r)}{\mathrm{d}r} = \frac{x_{n+1}-x_n}{2} = \frac{h_n}{2}, \tag{2.4}$$

where h_n is the length of element Ω_n. Using this mapping, we write (2.2a) and (2.2b) in the computational domain as

$$\frac{\partial u_n}{\partial t} = b\frac{1}{J_n}\nabla_r q_n, \tag{2.5a}$$

$$q_n = \frac{1}{J_n}\nabla_r u_n, \tag{2.5b}$$

where $\nabla_r = \frac{\partial}{\partial r}$.

Equations (2.5a) and (2.5b) are insufficient to describe the phenomenon occuring in the entire domain. To take into account the transfer of information between the cells, we must add a numerical flux to each equation. In this article, we will focus on the IP and BR2 numerical fluxes. We note $(u)^*$ as the numerical flux associated to the auxiliary equation and $(q)^*$ as the numerical flux associated to the primary equation. We then express (2.5a) and (2.5b) as

$$\frac{\partial u_n}{\partial t} = b\frac{1}{J_n}\nabla_r \left[q + (q_n^* - q_n)|_{-1}\, h_L + (q_n^* - q_n)|_1\, h_R\right], \tag{2.6a}$$

$$q_n = \frac{1}{J_n}\nabla_r \left[u_n + (u^* - u_n)|_{-1}\, g_L + (u^* - u_n)|_1\, g_R\right], \tag{2.6b}$$

where h_L and h_R are the FR correction functions, defined in the computational space, for respectively the left and right boundaries of the primary equation, while g_L and g_R are the corresponding correction functions for the auxiliary equation.

The main idea of these correction functions is to create continuous quantities through the edges of the element. Indeed, u is usually discontinuous between elements Ω_n and Ω_{n+1}. By adding the correction $(u^* - u_n)|_1 g_R$ to the solution u_n on the element Ω_n and the correction $(u^* - u_{n+1})|_{-1} g_L$ to the solution u_{n+1} on the element Ω_{n+1}, we obtain a continuous quantity u on $\Omega_n \cup \Omega_{n+1}$. A similar procedure is done for the quantity q in the primary equation. To create these continuous quantities, the correction functions g_L (respectively, g_R) and h_L (respectively, h_R) must respect particular features [10],

$$g_L(-1) = g_R(1) = 1, \tag{2.7a}$$

$$g_R(-1) = g_L(1) = 0, \tag{2.7b}$$

and h_L and h_R respect the same properties. Moreover, the correction functions g_L (respectively, g_R) and h_L (respectively, h_R) are polynomials of degree $p+1$. Indeed, as we will see shortly the solution at the time t_n, $u_n^{t_n}$, is a polynomial of degree p and therefore, for $u_n^{t_n+1}$ to be also a polynomial of degree p, we require the correction functions to be polynomials of degree $p+1$.

However, just respecting the above stated properties does not ensure the stability of the scheme. For the advection equation, Vincent, Castonguay, and Jameson defined a class (VCJH) of correction functions [19]; if the correction function g_L (similarly, g_R) satisfies the following property (see [19, equation (3.32)]), then the scheme is energy stable for the advection equation, using the Lax–Friedrichs numerical flux

$$\int_{-1}^{1} g_L \frac{\partial l_i}{\partial r}\mathrm{d}r = c\left(\frac{\partial^p l_i}{\partial r^p}\right)\left(\frac{\partial^{p+1} g_L}{\partial r^{p+1}}\right), \tag{2.8}$$

where c is a scalar and l_i is a Lagrange polynomial, which will be defined shortly. For $c \in [c_-, \infty[$, the corresponding correction function g provides a stable scheme for the advection equation. c_- is a negative value, given in [19].

The goal of this article is to obtain a stability condition for the advection-diffusion problem. Choosing the ESFR correction function only ensures the stability for the advection part. A new condition on the correction function for the diffusion term must be developed to ensure a stable scheme.

The diffusion equation combines both the auxiliary and primary equations and thus requires two correction functions g_L (respectively, g_R) and h_L (respectively, h_R), where both ESFR correction functions are parametrized by a different scalar: c for the h correction function and κ for the g correction function.

Numerically, we do not require the analytical formulation of g_L (respectively, g_R) and h_L (respectively, h_R) but of their derivatives. The final expression for the one-dimensional diffusion equation reads

$$\frac{\partial u_n}{\partial t} = b\frac{1}{J_n}\left[\nabla_r q_n + (q^* - q_n)|_{-1}\,\nabla_r h_L + (q^* - q_n)|_1\,\nabla_r h_R\right], \tag{2.9a}$$

$$q_n = \frac{1}{J_n}\left[\nabla_r u_n + (u^* - u_n)|_{-1}\,\nabla_r g_L + (u^* - u_n)|_1\,\nabla_r g_R\right], \tag{2.9b}$$

where $\nabla_r g$ and $\nabla_r h$ are the derivatives in the computational space.

To complete the formulation, it remains to describe the numerical fluxes for the choosen schemes. We will present the LDG [8], the IP [1], the BR2 [2], the CDG [14], and the CDG2 [3] numerical fluxes.

(2.10)

$$\begin{cases}\text{LDG:}\\ u^* = \{\!\{u\}\!\} - \beta[\![u]\!],\\ q^* = \{\!\{q\}\!\} + \beta[\![q]\!] - \tau[\![u]\!],\end{cases}\quad \begin{cases}\text{IP:}\\ u^* = \{\!\{u\}\!\},\\ q^* = \{\!\{\nabla u\}\!\} - \tau[\![u]\!],\end{cases}\quad \begin{cases}\text{BR2:}\\ u^* = \{\!\{u\}\!\},\\ q^* = \{\!\{\nabla u\}\!\} + s\{\!\{r^e\left([\![u]\!]\right)\}\!\},\end{cases}$$

$$\begin{cases}\text{CDG:}\\ u^* = \{\!\{u\}\!\} - \beta[\![u]\!],\\ q^* = \{\!\{\nabla u\}\!\} + \beta[\![\nabla u]\!] - \tau[\![u]\!] + \gamma L^e\left(u\right),\end{cases}\quad \begin{cases}\text{CDG2:}\\ u^* = \{\!\{u\}\!\},\\ q^* = \{\!\{\nabla u\}\!\} - \tau[\![u]\!] + \gamma L^e\left(u\right).\end{cases}$$

In the LDG and CDG approaches, β is a scalar value, in one dimension, while τ signifies the penalty term for both LDG and IP, s denotes the penalty term for the BR2 approach, and γ denotes the penalty term for the CDG/CDG2 formulation. The term r^e is a lifting operator and is defined as

$$\int_\Omega r^e\left([\![u]\!]\right)\phi\,\mathrm{d}x = -\int_e [\![u]\!]\{\!\{\phi\}\!\}\,\mathrm{d}s, \tag{2.11}$$

which can be written in one dimension as

$$\int_\Omega r^e\left([\![u]\!]\right)\phi\,\mathrm{d}x = -[\![u_e]\!]\{\!\{\phi_e\}\!\}, \tag{2.12}$$

where ϕ is a test function. The symbol $[\![\ ]\!]$ denotes a jump (it must not be confused with the integer interval $[\![.,.]\!]$) and $\{\!\{\}\!\}$ a mean value. The former notation defines the discontinuity of the solution across an edge, while the latter signifies the average of the solution across an edge. Last, L^e is a lifting operator and is defined as

$$L^e\left(u\right) = \{\!\{r^e\left([\![u]\!]\right)\}\!\} + \{\!\{l^e\left(\beta\left([\![u]\!]\right)\right)\}\!\} + \beta\left([\![r^e\left([\![u]\!]\right)]\!] + [\![l^e\left(\beta[\![u]\!]\right)]\!]\right), \tag{2.13}$$

where

$$\int_\Omega l^e\left(\beta[\![u]\!]\right)\phi\,\mathrm{d}x = -\beta[\![u_e]\!][\![\phi_e]\!]. \tag{2.14}$$

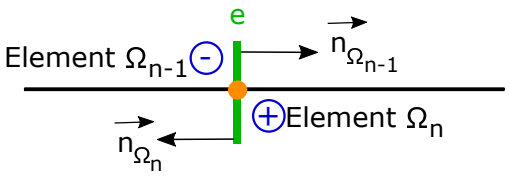

FIG. 1. *Normal vector convention on an edge.*

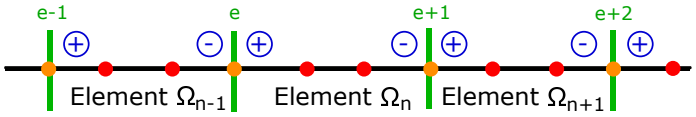

FIG. 2. *Representation of several elements for* $p = 1$.

Typically, the quantity u on the left side of an edge e is referred as $u_{e,-}$ and on the right side of the edge as $u_{e,+}$. Referring to Figure 1, we can define the jump and the mean value as

$$[\![u_e]\!] = u_{e,-} - u_{e,+}, \tag{2.15}$$

$$\{\!\{u_e\}\!\} = \frac{1}{2}\left(u_{e,-} + u_{e,+}\right). \tag{2.16}$$

Figure 2 describes the interface e located between elements Ω_{n-1} and Ω_n. For instance, $u_{e,-}$ represents the value taken by the solution on the element Ω_{n-1} on its right edge (green square on edge e), whereas $u_{e,+}$ represents the value taken by the solution on the element Ω_n on its left edge (green square on edge e). The red circles represent the $p+1$ solution points within any standard element, while the green square denotes the flux points. Indeed the solution on an element Ω_n will be calculated at N_p solution nodes within the element. Using Lagrange polynomials we can interpolate the solution with a polynomial of degree $p = N_p - 1$. The nodes, r_i, are typically chosen as the Lobatto–Gauss–Legendre (LGL) or the Gauss–Legendre (GL) nodes. Finally the solution u_n on the element Ω_n can be written as

$$u_n = \sum_{i=1}^{N_p} \hat{u}_i l_i, \tag{2.17}$$

where $\hat{u}_i$ is the value of u at the nodes r_i and l_i is the associated Lagrange polynomial,

$$l_i(r) = \prod_{\substack{j=1 \\ j \neq i}}^{N_P} \left(\frac{r - r_j}{r_i - r_j}\right). \tag{2.18}$$

The choice of the basis does not impact the results of the following sections. For numerical simulations, we used the Lagrangian basis. The number of nodes N_p and hence the degree of the polynomial p are of the utmost importance as with high-order methods we should get an error of order $\mathcal{O}(h^{p+1})$ in the L_2 norm, where h is a typical

TABLE 1
Numerical values of the correction function parameter for four particular methods.

c \ p	2	3	4	5
c_{DG}	0	0	0	0
c_{SD}	2.96e-02	9.52e-04	1.61e-05	1.70e-07
c_{HU}	6.67e-02	1.69e-03	2.52e-05	2.44e-07
c_+	1.86e-01	3.67e-03	4.79e-05	4.24e-07

element size. We have

$$\|u\|_{0,\Omega} = \left[\int_\Omega u^2 \,\mathrm{d}x\right]^{1/2}, \tag{2.19}$$

the L_2 norm of u.

In summary, we can enumerate the different choices available for the FR scheme as follows:

1. The choice of the correction functions g_L and g_R is established through the parameter κ. As we will show in the following section, the method is independent of κ when employing the IP or the BR2 numerical flux. This theoretical result will be verified for two values of κ, κ_{DG} and κ_+, which are particular values explained below. This article also contains the results of the LDG numerical flux. For this scheme, κ will have a wide range of values: $\kappa \in [0, 10^8]$.
2. The choice of the correction functions h_L and h_R is established through the parameter c. These correction functions pertain to the advective term, if there is one. Many studies have been conducted for the pure advective equation. In the dissertation of Castonguay [6], it was shown that for too large a value of c, we lose OOA. A particular value of c noted c_+ was defined as the parameter providing the maximal time step $\Delta t_{\max}$ while preserving the OOA. Therefore, in our analysis, we will mainly focus on a range of c in $[0, c_+]$. In this paper we will present three particular schemes: DG, SD, and HU (g_2 method). For brevity, their analytical expressions will not be given, only the numerical values. One can find them in the paper of Vincent, Castonguay, and Jameson [18].
   Although the three first rows of Table 1 are obtained by analytical formulas, the fourth row, corresponding to c_+, is obtained via a von Neumann analysis for the RK54 scheme [5]. These values are a bit different from the one obtained by Vincent, Castonguay, and Jameson [18]. We suspect numerical approximations to be the source of these discrepancies.
3. The choice of number and position of nodes. Although the simulations have been done for equidistant GL and LGL points, only the results of LGL will be presented for brevity, since the trends are similar. The degree of the polynomial has been taken to be $[\![2, 5]\!]$, but only $p = 2$ and $p = 3$ will be presented. Results for all other p demonstrated similar trends.
4. The penalty term τ for the IP numerical fluxes, s for the BR2 numerical fluxes, β for the LDG/CDG numerical fluxes, and γ for the CDG/CDG2 numerical fluxes.

3. The diffusion equation, independent of κ. The purpose of this section is to prove that using the ESFR schemes with the compact numerical fluxes (IP, BR2,

CDG, and CDG2 approaches) results in an independency of the problem from κ. We will use the CDG scheme as it is the most general.

The CDG numerical fluxes described in (2.10) yield for an element Ω_n

$$(u^* - u_n)|_{-1} = [\![u_e]\!] \left(\frac{1}{2} - \beta\right), \tag{3.1}$$

$$(u^* - u_n)|_{1} = -[\![u_{e+1}]\!] \left(\frac{1}{2} + \beta\right). \tag{3.2}$$

We retrieve the equivalent terms for the IP, BR2, and CDG2 numerical fluxes by taking $\beta = 0$. The compact schemes differ also by their definition of q^*. For more generality, we will not replace q^* by its expression in the following derivations.

We introduce the previous equalities in (2.9a) and (2.9b),

$$\frac{\partial u_n}{\partial t} = b\frac{1}{J_n}\left[\nabla_r q_n + (q^* - q_n)|_{-1} \nabla_r h_L + (q^* - q_n)|_{1} \nabla_r h_R\right], \tag{3.3a}$$

$$q_n = \frac{1}{J_n}\left[\nabla_r u_n + [\![u_e]\!] \left(\frac{1}{2} - \beta\right) \nabla_r g_L - [\![u_{e+1}]\!] \left(\frac{1}{2} + \beta\right) \nabla_r g_R\right]. \tag{3.3b}$$

We now substitute (3.3b) into (3.3a),

$$\begin{aligned}\frac{\partial u_n}{\partial t} = {} & \frac{b}{J_n}\left[\frac{1}{J_n}\Delta_r u_n + \left(q^* - \frac{1}{J_n}\nabla_r u_n\right)\Big|_{-1} \nabla_r h_L + \left(q^* - \frac{1}{J_n}\nabla_r u_n\right)\Big|_{1} \nabla_r h_R\right] \\ & + \frac{b[\![u_e]\!]}{J_n^2}\left(\frac{1}{2} - \beta\right)\left[\Delta_r g_L - \nabla_r g_L(-1)\nabla_r h_L - \nabla_r g_L(1)\nabla_r h_R\right] \\ & - \frac{b[\![u_{e+1}]\!]}{J_n^2}\left(\frac{1}{2} + \beta\right)\left[\Delta_r g_R - \nabla_r g_R(-1)\nabla_r h_L - \nabla_r g_R(1)\nabla_r h_R\right],\end{aligned} \tag{3.4}$$

where $\Delta_r = \frac{\partial^2}{\partial r^2}$. The first line of (3.4) does not depend on κ, but the last two contain the correction function, g, and hence could potentially depend on κ.

THEOREM 3.1. *Employing the ESFR correction functions defined in Definitions* B.1 *and* B.2, *the following expression is independent of* κ*:*

$$\Delta_r g_L - \nabla_r g_L(-1)\nabla_r h_L - \nabla_r g_L(1)\nabla_r h_R, \tag{3.5}$$

where g_L *and* g_R *are parametrized by* κ *and* h_L *and* h_R *by c.*

Proof. In the following derivations, the authors have used the properties of the Legendre polynomials, which are recalled in Appendix A. From Definition B.1 of the left ESFR correction function and from Property A.1, we have

$$\begin{aligned}\nabla_r g_L(-1) &= \frac{(-1)^p}{2}\left[\frac{(-1)^{p+1} p(p+1)}{2} - \frac{\eta_{p,\kappa}(-1)^p p(p-1) + (-1)^p (p+1)(p+2)}{2(1+\eta_{p,\kappa})}\right] \\ &= -\frac{1}{4}\left[p(p+1) + \frac{\eta_{p,\kappa} p(p-1) + (p+1)(p+2)}{(1+\eta_{p,\kappa})}\right].\end{aligned} \tag{3.6}$$

Similarly, we obtain

$$\nabla_r g_L(1) = \frac{(-1)^p}{4}\left[p(p+1) - \frac{\eta_{p,\kappa} p(p-1) + (p+1)(p+2)}{(1+\eta_{p,\kappa})}\right]. \tag{3.7}$$

We now multiply the previous equations by $\nabla_r h_L$ (respectively, $\nabla_r h_R$),

(3.8a)
$$\nabla_r g_L\,(-1)\,\nabla_r h_L = \frac{(-1)^p}{8}\left[p\,(p+1)+\frac{\eta_{p,\kappa}p(p-1)+(p+1)(p+2)}{(1+\eta_{p,\kappa})}\right]\left(-\Psi_p^{'}+\frac{\eta_{p,c}\Psi_{p-1}^{'}+\Psi_{p+1}^{'}}{(1+\eta_{p,c})}\right),$$

(3.8b)
$$\nabla_r g_L(1)\nabla_r h_R = \frac{(-1)^p}{8}\left[p(p+1)-\frac{\eta_{p,\kappa}p(p-1)+(p+1)(p+2)}{(1+\eta_{p,\kappa})}\right]\left(\Psi_p^{'}+\frac{\eta_{p,c}\Psi_{p-1}^{'}+\Psi_{p+1}^{'}}{(1+\eta_{p,c})}\right),$$

where $\Psi_p^{'}$ denotes the derivative of the Legendre polynomial of degree p.

Then, we add the above two equations to yield

(3.9)
$$\nabla_r g_L\,(-1)\,\nabla_r h_L+\nabla_r g_L\,(1)\,\nabla_r h_R=\frac{(-1)^p}{4}p\,(p+1)\left(\frac{\eta_{p,c}\Psi_{p-1}^{'}+\Psi_{p+1}^{'}}{(1+\eta_{p,c})}\right)+\frac{(-1)^{p+1}}{4}\left(\frac{\eta_{p,\kappa}p\,(p-1)+(p+1)\,(p+2)}{(1+\eta_{p,\kappa})}\Psi_p^{'}\right).$$

Next, we shift our focus to the Laplacian of the correction function; differentiating Property A.3 with respect to r yields,

(3.10)
$$\begin{aligned}\Delta_r g_L &= \frac{(-1)^p}{2}\left[\Psi_p^{''}-\frac{\eta_{p,\kappa}\Psi_{p-1}^{''}+\Psi_{p+1}^{''}}{(1+\eta_{p,\kappa})}\right]\\ &= \frac{(-1)^p}{2}\left[\Psi_p^{''}-\Psi_{p-1}^{''}-\frac{(2p+1)\,\Psi_p^{'}}{(1+\eta_{p,\kappa})}\right].\end{aligned}$$

By substracting (3.9) from (3.10), we obtain

(3.11)
$$\begin{aligned}&\Delta_r g_L-\left(\nabla_r g_L\,(-1)\,\nabla_r h_L+\nabla_r g_L\,(1)\,\nabla_r h_R\right)\\ &\quad=\frac{(-1)^p}{2}\left[\Psi_p^{''}-\Psi_{p-1}^{''}\right]\\ &\qquad+\frac{(-1)^{p+1}}{4}p\,(p+1)\left(\frac{\eta_{p,c}\Psi_{p-1}^{'}+\Psi_{p+1}^{'}}{(1+\eta_{p,c})}\right)\\ &\qquad+\frac{(-1)^p}{4}\left(\frac{\eta_{p,\kappa}p\,(p-1)+(p+1)\,(p+2)-2\,(2p+1)}{(1+\eta_{p,\kappa})}\Psi_p^{'}\right)\\ &\quad=\frac{(-1)^p}{2}\left[\Psi_p^{''}-\Psi_{p-1}^{''}\right]\\ &\qquad+\frac{(-1)^{p+1}}{4}p\,(p+1)\left(\frac{\eta_{p,c}\Psi_{p-1}^{'}+\Psi_{p+1}^{'}}{(1+\eta_{p,c})}\right)\\ &\qquad+\frac{(-1)^p}{4}p\,(p-1)\,\Psi_p^{'},\end{aligned}$$

where the final form only contains $\eta_{p,c}$. ∎

Remark 3.2. The same property can be said for

$$\Delta_r g_R - \nabla_r g_R\,(-1)\,\nabla_r h_L - \nabla_r g_R\,(1)\,\nabla_r h_R;$$

we need only to adapt the previous proof to g_R.

THEOREM 3.3. *The discretized diffusion equation is independent of κ when employing compact numerical fluxes within the ESFR framework.*

Proof. The diffusion equation with the ESFR schemes and employing the IP, BR2, CDG, or CDG2 numerical fluxes is written as (3.4). Only the last two lines of this PDE contain the parameter κ. However, from Theorem 3.1 and Remark 3.2 the parameter κ gets simplified and as a consequence (3.4) does not depend on κ. ∎

4. Energy stability condition for compact schemes.

4.1. General theoretical result. Having introduced the different notation and definitions, we can derive the stability condition for the IP numerical flux using the ESFR class of correction functions. We will, briefly, explain the main result of [7] for the LDG numerical fluxes and explain how, from this analysis, we can extend the proof. The main difference between the notation of [7] and ours is that we have dropped the superscript $-^D$ which indicated "discontinuous" quantities. Castonguay et al. derived a stability condition for the LDG numerical flux [7] by introducing the norms

$$\|U\|_{p,c} = \left\{ \sum_{n=1}^{N_K} \int_{x_n}^{x_{n+1}} \left[(u_n)^2 + \frac{c}{2} (J_n)^{2p} \left(\frac{\partial^p u_n}{\partial x^p} \right)^2 \right] \mathrm{d}x \right\}^{1/2} \tag{4.1}$$

and

$$\|Q\|_{p,\kappa} = \left\{ \sum_{n=1}^{N_K} \int_{x_n}^{x_{n+1}} \left[(q_n)^2 + \frac{\kappa}{2} (J_n)^{2p} \left(\frac{\partial^p q_n}{\partial x^p} \right)^2 \right] \mathrm{d}x \right\}^{1/2}. \tag{4.2}$$

These norms are used to obtain particular properties of the correction functions g and h and thus drastically simplify the equations of stability. After applying the simplifications, they showed for the LDG case [7, equation (77)] that

$$\frac{1}{2}\frac{\mathrm{d}}{\mathrm{d}t}\|U\|_{p,c}^2 = -b\|Q\|_{p,\kappa}^2 - \sum_{e=1}^{N_e} \left[\frac{\lambda}{2}|a|\,(u_{e,+} - u_{e,-})^2 + \tau\,(u_{e,+} - u_{e,-})^2 \right], \tag{4.3}$$

where N_e is the number of edges, λ is the parameter of the Lax–Friedrichs numerical flux, and a is the velocity of the advection.

The conclusion of their stability proof is that for all $\lambda \geq 0$ and $\tau \geq 0$,

$$\frac{1}{2}\frac{\mathrm{d}}{\mathrm{d}t}\|U\|_{p,c}^2 \leq 0. \tag{4.4}$$

From this final result (4.3), it is important to notice that the advective part, represented by $\frac{\lambda}{2}|a|(u_{e,+} - u_{e,-})^2$, is independent from the diffusive part $\tau(u_{e,+} - u_{e,-})^2$. Therefore, by taking any other diffusive scheme, the advective part will not change. In order for our proof to be as concise as possible, we will not consider the advective part (as it will not differ from the article of Castonguay et al.). Due to the similarities with [7], the authors have chosen not to re-derive every step of the

derivations. We will start from a particular equation of the aforementioned article. To have a complete understanding of the proof, the authors strongly recommend reading article [7] (up to equation (69)), which has been derived for any diffusive numerical flux.

Upon removing the advective term of [7, equation (69)] we have

$$\frac{1}{2}\frac{\mathrm{d}}{\mathrm{d}t}\|U\|_{p,c}^2 = -b\|Q\|_{p,\kappa}^2 + b\sum_{e=1}^{N_e}\Theta_e, \tag{4.5}$$

where $\Theta_e = [(u_{e,+}q_{e,+} - u_{e,-}q_{e,-}) - (q)_e^*(u_{e,+} - u_{e,-}) - (u)_e^*(q_{e,+} - q_{e,-})]$. Since the diffusive parameter b is a positive constant and multiplies every term, we have factored it out from Θ_e. This is a slight difference from equation (75) in [7], where b does not multiply the penalty term. The choice made here does not impact the result of this article. In the following derivations, we will use the CDG numerical fluxes with $\gamma = 0$. As we will show in the next section the term $\gamma L^e(u)$ is equivalent to a constant scalar multiplied by $[\![u_e]\!]$. Therefore as long as we consider the term $\tau[\![u_e]\!]$ (which can include the term $\gamma L^e(u)$), we can consider $\gamma = 0$ without loss of generality.

LEMMA 4.1. *Employing the ESFR correction functions and the CDG approach with $\gamma = 0$, the following equality holds:*

$$\begin{aligned}\Theta_e = &-[\![u_e]\!]^2\left[\tau + \frac{1}{4}\nabla_r g_L(-1)\left(\frac{(1+4\beta(1+\beta))}{J_{n-1}} + \frac{(1-4\beta(1-\beta))}{J_n}\right)\right]\\ &- \frac{1}{4}\nabla_r g_L(1)[\![u_e]\!]\left(\frac{(1-4\beta^2)}{J_{n-1}}[\![u_{e-1}]\!] + \frac{(1-4\beta^2)}{J_n}[\![u_{e+1}]\!]\right).\end{aligned} \tag{4.6}$$

Proof. We expand the expression for Θ_e by employing the CDG numerical fluxes defined in (2.10) with $\gamma = 0$,

$$\begin{aligned}\Theta_e = &(u_{e,+}q_{e,+} - u_{e,-}q_{e,-})\\ &- (\{\!\{\nabla u_e\}\!\} + \beta[\![\nabla u_e]\!] - \tau[\![u_e]\!])(u_{e,+} - u_{e,-}) - (\{\!\{u_e\}\!\} - \beta[\![u_e]\!])(q_{e,+} - q_{e,-}).\end{aligned} \tag{4.7}$$

By expanding the mean value, defined in (2.16), and using the definition of the jump from (2.15), we obtain

$$\begin{aligned}\Theta_e &= (u_{e,+}q_{e,+} - u_{e,-}q_{e,-}) + (\{\!\{\nabla u_e\}\!\} + \beta[\![\nabla u_e]\!] - \tau[\![u_e]\!])[\![u_e]\!]\\ &\quad - \left(\frac{1}{2}u_{e,+} + \frac{1}{2}u_{e,-}\right)(q_{e,+} - q_{e,-}) - \beta[\![u_e]\!][\![q_e]\!]\\ &= u_{e,+}q_{e,+}\left(1 - \frac{1}{2}\right)\\ &\quad + u_{e,+}q_{e,-}\left(\frac{1}{2}\right)\\ &\quad + u_{e,-}q_{e,-}\left(-1 + \frac{1}{2}\right)\\ &\quad + u_{e,-}q_{e,+}\left(-\frac{1}{2}\right)\\ &\quad + (\{\!\{\nabla u_e\}\!\} + \beta[\![\nabla u_e]\!] - \tau[\![u_e]\!])[\![u_e]\!] - \beta[\![u_e]\!][\![q_e]\!].\end{aligned} \tag{4.8}$$

Using once more the definition of the mean value and the jump, we reduce the expression to

$$\begin{aligned}\Theta_e &= u_{e,+}\{\!\{q_e\}\!\} - u_{e,-}\{\!\{q_e\}\!\} + \{\!\{\nabla u_e\}\!\}[\![u_e]\!] - \beta[\![u_e]\!][\![q_e]\!] + \beta[\![u_e]\!][\![\nabla u_e]\!] - \tau[\![u_e]\!]^2 \\ &= -[\![u_e]\!]\{\!\{q_e - \nabla u_e\}\!\} + \beta[\![u_e]\!]\left([\![\nabla u_e - q_e]\!]\right) - \tau[\![u_e]\!]^2.\end{aligned} \tag{4.9}$$

In order to simplify (4.9), we write the auxiliary variable (equation (2.9b)), for an element Ω_n, in terms of u and use the relations (3.3a) and (3.3b),

$$q_n = \nabla u_n + \frac{1}{J_n}[\![u_e]\!]\left(\frac{1}{2} - \beta\right)\nabla_r g_L - \frac{1}{J_n}[\![u_{e+1}]\!]\left(\frac{1}{2} + \beta\right)\nabla_r g_R, \tag{4.10}$$

where q and ∇u are in the physical space, while $\nabla_r g_L$ and $\nabla_r g_R$ are in the computational space. Therefore, referring to Figure 2, we have

$$q_{e,+} = \nabla u_{e,+} + \frac{1}{J_n}[\![u_e]\!]\left(\frac{1}{2} - \beta\right)\nabla_r g_L(-1) - \frac{1}{J_n}[\![u_{e+1}]\!]\left(\frac{1}{2} + \beta\right)\nabla_r g_R(-1), \tag{4.11a}$$

$$q_{e,-} = \nabla u_{e,-} + \frac{1}{J_{n-1}}[\![u_{e-1}]\!]\left(\frac{1}{2} - \beta\right)\nabla_r g_L(1) - \frac{1}{J_{n-1}}[\![u_e]\!]\left(\frac{1}{2} + \beta\right)\nabla_r g_R(1). \tag{4.11b}$$

Therefore, in (4.9) the gradient of the solution is simplified and we acquire

$$\begin{aligned}\Theta_e = &-\frac{1}{4}[\![u_e]\!]\Bigg[[\![u_e]\!]\left(\frac{1}{J_n}\nabla_r g_L(-1) - \frac{1}{J_{n-1}}\nabla_r g_R(1)\right) \\ &\qquad + \frac{1}{J_{n-1}}[\![u_{e-1}]\!]\nabla_r g_L(1) - \frac{1}{J_n}[\![u_{e+1}]\!]\nabla_r g_R(-1)\Bigg] \\ &+ \beta^2[\![u_e]\!]\left(\frac{\nabla_r g_L(1)}{J_{n-1}}[\![u_{e-1}]\!] - \frac{\nabla_r g_R(-1)}{J_n}[\![u_{e+1}]\!]\right) \\ &+ \beta[\![u_e]\!]^2\left(\frac{\nabla_r g_R(1)}{J_{n-1}}(1+\beta) + \frac{\nabla_r g_L(-1)}{J_n}(1-\beta)\right) - \tau[\![u_e]\!]^2.\end{aligned} \tag{4.12}$$

We finally use Theorem B.3 and replace $\nabla_r g_R(1)$ and $\nabla_r g_R(-1)$, respectively, by $-\nabla_r g_L(-1)$ and $-\nabla_r g_L(1)$ to obtain (4.6),

$$\begin{aligned}\Theta_e = &-[\![u_e]\!]^2\left[\tau + \frac{1}{4}\nabla_r g_L(-1)\left(\frac{1}{J_{n-1}} + \frac{1}{J_n}\right) - \beta\nabla_r g_L(-1)\left(\frac{-(1+\beta)}{J_{n-1}} + \frac{(1-\beta)}{J_n}\right)\right] \\ &- \frac{1}{4}\nabla_r g_L(1)[\![u_e]\!]\left(\frac{1}{J_{n-1}}[\![u_{e-1}]\!] + \frac{1}{J_n}[\![u_{e+1}]\!]\right) \\ &+ \beta^2\nabla_r g_L(1)[\![u_e]\!]\left(\frac{1}{J_{n-1}}[\![u_{e-1}]\!] + \frac{1}{J_n}[\![u_{e+1}]\!]\right).\end{aligned}$$

∎

Remark 4.2. We clearly see from (4.9) that if we had taken the LDG formulation, then ∇u_e would have been replaced by q_e. We would have then recovered the result of [7]: $\Theta_e = -\tau[\![u_e]\!]^2$.

THEOREM 4.3. *Employing the CDG numerical fluxes with $\gamma = 0$ for the diffusion equation with the ESFR schemes, τ_e greater than τ_e^* implies the energy stability, with*

$$\begin{aligned}\tau_{e,1}^* = \frac{1}{4}\Bigg[&|\nabla_r g_L(1)| \left(\frac{\left|1-4\beta^2\right|}{J_{n-1}} + \frac{\left|1-4\beta^2\right|}{J_n} \right) \\ &- \nabla_r g_L(-1) \left(\frac{(1+4\beta(1+\beta))}{J_{n-1}} + \frac{(1-4\beta(1-\beta))}{J_n} \right) \Bigg].\end{aligned} \tag{4.13}$$

Proof. We apply the triangular inequality ($2ab \le a^2 + b^2$) with $a = [\![u_e]\!]$ and $b = [\![u_{e-1}]\!]$ or $b = [\![u_{e+1}]\!]$ to the last term of (4.6). We do not know the sign of the quantity $\nabla_r g_L(1)$ as well as the sign of $(1-4\beta^2)$; therefore we need to place these terms within an absolute value and the triangle inequality yields

$$\begin{cases} -\dfrac{\left(1-4\beta^2\right)}{4J_{n-1}} \nabla_r g_L(1) [\![u_e]\!][\![u_{e-1}]\!] \le \dfrac{\left|1-4\beta^2\right|}{8J_{n-1}} |\nabla_r g_L(1)| \left([\![u_e]\!]^2 + [\![u_{e-1}]\!]^2 \right), \\ -\dfrac{\left(1-4\beta^2\right)}{4J_n} \nabla_r g_L(1) [\![u_e]\!][\![u_{e+1}]\!] \le \dfrac{\left|1-4\beta^2\right|}{8J_n} |\nabla_r g_L(1)| \left([\![u_e]\!]^2 + [\![u_{e+1}]\!]^2 \right). \end{cases} \tag{4.14}$$

Introducing these inequalities into (4.6), we retrieve

$$\begin{aligned}\Theta_e \le -[\![u_e]\!]^2 \Bigg[&\tau + \frac{1}{4}\nabla_r g_L(-1) \left(\frac{(1+4\beta(1+\beta))}{J_{n-1}} + \frac{(1-4\beta(1-\beta))}{J_n} \right) \\ &- \frac{1}{8}|\nabla_r g_L(1)| \left(\frac{\left|1-4\beta^2\right|}{J_{n-1}} + \frac{\left(1-4\beta^2\right|}{J_n} \right) \Bigg] \\ &+ \frac{1}{8}|\nabla_r g_L(1)| \left(\frac{\left|1-4\beta^2\right|}{J_{n-1}} [\![u_{e-1}]\!]^2 + \frac{\left|1-4\beta^2\right|}{J_n} [\![u_{e+1}]\!]^2 \right).\end{aligned} \tag{4.15}$$

Next, we sum over all the edges, and for simplicity, we consider Dirichlet conditions (periodic boundaries conditions work as well). Therefore, on the first and last elements, the jump associated is equal to 0. We notice that Θ_e depends on the jump at edges e, $e+1$ and $e-1$. Therefore Θ_{e+1} and Θ_{e-1} will have a contribution of $\frac{1}{8}|\nabla_r g_L(1)|$ to the term $[\![u_e]\!]^2$ each. We thus finally obtain the stability condition for the IP numerical fluxes,

$$\begin{aligned}\sum_{e=1}^{N_e} \Theta_e \le -\sum_{e=1}^{N_e} [\![u_e]\!]^2 \Bigg[&\tau + \frac{1}{4}\nabla_r g_L(-1) \left(\frac{(1+4\beta(1+\beta))}{J_{n-1}} + \frac{(1-4\beta(1-\beta))}{J_n} \right) \\ &- \frac{1}{4}|\nabla_r g_L(1)| \left(\frac{\left|1-4\beta^2\right|}{J_{n-1}} + \frac{\left|1-4\beta^2\right|}{J_n} \right) \Bigg].\end{aligned} \tag{4.16}$$

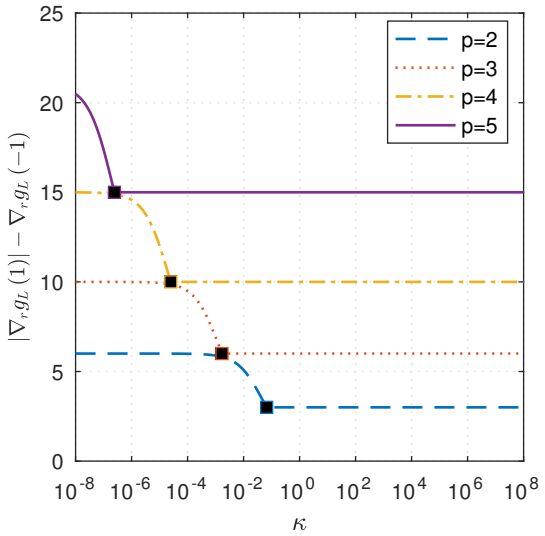

FIG. 3. $|\nabla_r g_L(1)| - \nabla_r g_L(-1)$ *for different values of* κ *and* p. *The black squares denote the value obtained with* $\kappa_{\min}$.

We may thus conclude that to ensure energy stability for the diffusion equation in one dimension for the CDG ($\gamma = 0$) formulation we require for every edge e,

$$\tau_e \geq \tau_{e,1}^* \implies \sum_{e=1}^{N_e} \Theta_e \leq 0 \implies \frac{\mathrm{d}}{\mathrm{d}t}\|U\|_{p,c}^2 \leq 0, \tag{4.17}$$

with, $\tau_{e,1}^*$ defined in (4.13).

Now from the result of Theorem 3.3, we know that the ESFR schemes do not depend on κ. Therefore the stability condition shouldn't depend on κ either. We may sharpen the previous bound as

$$\tau_e \geq \tau_e^* = \min_{\kappa}\left(\tau_{e,1}^*\right). \tag{4.18}$$ ∎

4.2. IP energy stability condition.

THEOREM 4.4. *Employing the IP numerical fluxes for the diffusion equation with the ESFR schemes,* τ_e *greater than* $\tau_{IP,e}^*$ *implies the energy stability, with*

(4.19)

$$\tau_e \geq \tau_{IP,e}^* = \frac{1}{4}\left(\frac{1}{J_{n-1}} + \frac{1}{J_n}\right)\min_{\kappa}\left(|\nabla_r g_L(1)| - \nabla_r g_L(-1)\right) \ \forall e \in [\![1, N_e]\!] \implies \frac{d}{dt}\|U\|_{p,c}^2 \leq 0.$$

Proof. We apply Theorem 4.3 with $\beta = 0$. ∎

Remark 4.5. Trivial derivations showed that $\min_\kappa(|\nabla_r g_L(1)| - \nabla_r g_L(-1))$ is obtained for $\kappa_{\min} = \frac{2(p+1)}{p(2p+1)(a_p p!)^2}$ or any greater value, where a_p is given in Appendix B. Numerical simulations were conducted to verify this result and are represented in Figure 3. In the rest of the article $\tau_{IP,e}^*$ will be computed with this optimal value.

4.3. Numerical results. Several numerical simulations have been conducted to verify the result (4.19). For equally spaced elements ($J_n = J$) (2.6a) and (2.6b) can be written as follows for the IP numerical fluxes:

$$\begin{cases} \dfrac{\partial u}{\partial t} = \dfrac{b}{J}\left(\nabla_r q + \left(\dfrac{1}{J}\{\!\{\nabla_r u\}\!\} - q - \tau[\![u_e]\!]\right)\Big|_{-1} \nabla_r h_L \right. \\ \qquad\qquad \left. + \left(\dfrac{1}{J}\{\!\{\nabla_r u\}\!\} - q - \tau[\![u_e]\!]\right)\Big|_{1} \nabla_r h_R\right), \\ q = \dfrac{1}{J}\left(\nabla_r u + (\{\!\{u\}\!\} - u)|_{-1}\nabla_r g_L + (\{\!\{u\}\!\} - u)|_{1}\nabla_r g_R\right). \end{cases} \tag{4.20}$$

The purpose of this numerical simulation is to determine, numerically, the minimum penalization term τ required for stability. The problem solved is the following: find $u(x,t)$ such that

$$\begin{cases} \dfrac{\partial u}{\partial t} = b\Delta u & \text{for } x \in [0, 2\pi] \text{ and } t \in [0,2], \\ u(x,0) = \sin(x) + \cos(x). \end{cases} \tag{4.21}$$

We impose Dirichlet boundary conditions and the exact solution for this system is $u_{exact} = e^{-bt}(\sin(x) + \cos(x))$.

In order to assess the stability of the numerical experiment, we choose a criterion on the upper bound of the solution such that $|u(x,t)| \leq u_{\max}$, where $u_{\max}$ is an arbitrarily large and problem-dependent value. Here $u_{exact} \leq \sqrt{2}$ for all t; we hence choose $u_{\max} = 2$, i.e., sufficiently greater than $\sqrt{2}$, for the differences to be caused by numerical instabilities arising from the scheme. The procedure is as follows.

Algorithm 4.1 Obtain $\tau^*_{numerical}$ with a precision of 0.01.

$i \leftarrow 0$
$\mathrm{d}\tau_i \leftarrow 1$
$j \leftarrow 0$
$\tau_j \leftarrow \tau$
Choose τ to be sufficiently low such that the first iteration is unstable. For the IP approach, a negative value is sufficient (which is not the case for LDG: a negative penalty term may still provide a stable scheme).
while $i < 3$ **do**
  Compute $u(x,t)$ for $x \in [0, 2\pi]$ and $t \in [0,2]$. The final time $t = 2$ is chosen to ensure that a few thousand iterations are run
  if $\max|u(x,t)| \geq u_{\max}$ **then**
    $\tau_{j+1} \leftarrow \tau_j + \mathrm{d}\tau_i \;\; j \leftarrow j+1$
  else
    $\tau_{j+1} \leftarrow \tau_j - \mathrm{d}\tau_i$
    $\mathrm{d}\tau_i \leftarrow \mathrm{d}\tau_i/10$
    $i \leftarrow i+1$
  end if
end while

Through Algorithm 4.1, we achieve the minimal numerical penalization term: $\tau^*_{numerical}$ with a precision of $\mathrm{d}\tau_2 = 0.01$ for which we observe convergence. It is generally accepted that for $\tau \geq \tau^*_{numerical}$ we have stability but we may lose the

TABLE 2
$\tau^*_{IP,e}$ compared to $\tau^*_{numerical}$ for the IP formulation for $p = 2$ and $p = 3$, and 32 elements.

p	2					3				
$\tau^*_{IP,e}$	15.28	15.28	15.28	15.28	15.28	30.56	30.56	30.56	30.56	30.56
c \ κ	κ_{DG}	κ_{SD}	κ_{Hu}	κ_+	10^5	κ_{DG}	κ_{SD}	κ_{Hu}	κ_+	10^5
c_{DG}	15.21	15.21	15.21	15.21	15.21	30.49	30.49	30.49	30.49	30.49
c_{SD}	15.18	15.18	15.18	15.18	15.18	30.46	30.46	30.46	30.46	30.46
c_{HU}	15.12	15.12	15.12	15.12	15.12	30.43	30.43	30.43	30.43	30.43
c_+	14.97	14.97	14.68	14.97	14.97	30.35	30.35	30.35	30.35	30.35
10^5	5.02	5.02	5.02	5.02	5.02	15.21	15.21	15.21	15.21	15.21

performance of the method (conditioning of the matrix [16] and increased maximal time step; see section 6) if τ is too large.

We have several choices of parameters to conduct the simulations. For the results presented, we choose a diffusive parameter $b = 1$. The domain was discretized into $N_K = 32$ equally distributed elements (J is a constant throughout the domain). The time resolution solver is a five-stage, fourth-order Runge–Kutta method (RK54 introduced by Carpenter and Kennedy [5]). Since the purpose of this study is to find the minimal penalty term τ, we cannot immediately conduct a von Neumann analysis to find the maximal time step $\Delta t_{\max}$. Therefore, we select a time step recommended by Hesthaven and Warburton [12]: $\Delta t = \frac{1}{b} CFL \min(\Delta x)^2$ (in our cases $CFL = 0.05$). The maximum time step associated to a value of τ will be computed in section 6.

We conduct several experiments with the degree of the interpolation polynomial p as a parameter and employ the LGL points.

As we observed in (4.19) $\tau^*_{IP,e}$ depends only on the Jacobian J and on the degree of polynomial p. Hence it is independent of κ and c. The first line of entries in Table 2 corresponds to these theoretical values. The rest of the values correspond to the numerical values obtained via Algorithm 4.1. Two main observations can be made concerning the results in Table 2. First, we discern that the relationship $\tau^*_{IP,e} \geq \tau^*_{numerical}$ is respected. If we take any value of τ greater than the theoretical result, then we are guaranteed to achieve convergence. Second, as c decreases, $\tau^*_{numerical}$ approaches $\tau^*_{IP,e}$. The fact that $\tau^*_{numerical}$ is less than our theoretical results comes from our stability condition. We choose $\tau^*_{IP,e}$ such that $\sum_{e=}^{N_e} \Theta_e \leq 0$ in order to ensure $\frac{\mathrm{d}}{\mathrm{d}t}\|U\|^2_{p,c} \leq -b\|Q\|^2_{p,\kappa} + b\sum_{e=1}^{N_e} \Theta_e \leq 0$. In fact, a sufficient criterion for stability is just $\frac{\mathrm{d}}{\mathrm{d}t}\|U\|^2_{p,c} \leq 0$.

Therefore, to improve our results, we could have looked for a bound for τ such that

$$\sum_{e=1}^{N_e} \Theta_e \leq \|Q\|^2_{p,\kappa}. \tag{4.22}$$

The result, $\tau^*_{IP,e} \geq \tau^*_{numerical}$, confirms that there is yet to find a sharper inequality for τ. Moreover the norm of u chosen in (4.1) is stronger than just the energy stability. Indeed proving $\frac{\mathrm{d}}{\mathrm{d}t}\|u\|^2_{0,\Omega} \leq 0$ is sufficient to ensure stability.

Remark 4.6. Shahbazi [16] derived the coercivity of the Poisson equation for the DG method with the IP numerical fluxes. Adapted to a one-dimensional problem, his

result yields

$$\tau^* = \frac{3\,(p+1)^2}{2J}. \tag{4.23}$$

It can be easily shown that the coercivity of the Poisson equation implies the energy stability of the discrete diffusion equation. Hence the condition (4.23) also yields the ESFR stability for the FR-DG method. However, the stability condition found in (4.19) is more than three times sharper than (4.23) and is valid for any other ESFR schemes.

5. BR2, CDG, and CDG2 stability condition. The purpose of this section is to prove the equivalence between the IP and the BR2 numerical fluxes in one-dimensional problems and to give the stability condition for the CDG and CDG2 formulation. The equivalence between the IP and the BR2 approaches was suggested by Wang, Gao, and Haga [21]. Huynh established [11] a direct link between the derivative of the correction function and the lifting operator applied to recover the FR formulation from the DG formulation. For completness of the article, a short recall of the different steps is presented.

Let us consider the linear advection problem in one dimension.

$$\frac{\partial u}{\partial t} = -\nabla F, \tag{5.1}$$

where $F = au$ is the flux and a the velocity. Using the mapping defined in (2.3) and applying the DG method, in its strong formulation [12], results in

$$\sum_n \int_{-1}^{1} \frac{\partial u_n}{\partial t}\phi \,\mathrm{d}r = -\left(\int_{-1}^{1} \nabla_r F_n \phi \,\mathrm{d}r + \underbrace{\left[(F_n^* - F_n)(1)\phi(1) - (F_n^* - F_n)(-1)\phi(-1)\right]}_{\text{Terms to be lifted}}\right), \tag{5.2}$$

where ϕ is the test function, polynomial of degree less or equal to p and F^* is the numerical flux for the advection equation. Introducing g_L and g_R, such that

$$\int_{-1}^{1} \nabla_r g_L \phi \,\mathrm{d}r = -\phi\,(-1) \;\text{ and }\; \int_{-1}^{1} \nabla_r g_R \phi \,\mathrm{d}r = \phi\,(1)\,, \tag{5.3}$$

we then obtain from (5.2),

$$\sum_n \int_{-1}^{1} \left[\left(\frac{\partial u_n}{\partial t} + \nabla_r F_n + (F_n^* - F_n)\,(-1)\,\nabla_r g_L + (F_n^* - F_n)\,(1)\,\nabla_r g_R\right)\phi\right] = 0. \tag{5.4}$$

We have, for all elements Ω_n, the differential equation (FR method),

$$\frac{\partial u_n}{\partial t} = -\left[\nabla_r F_n + (F_n^* - F_n)\,(-1)\,\nabla_r g_L + (F_n^* - F_n)\,(1)\,\nabla_r g_R\right]. \tag{5.5}$$

As explained in section 2, both g_L and g_R are polynomials of degree $p+1$, hence $p+2$ conditions are required to define them properly.

LEMMA 5.1. *Employing the ESFR correction functions defined in Definitions* B.1 *and* B.2, *there exists a unique value of* κ *such that* (5.3) *are valid and this value is* $\kappa = 0$.

Proof. For brevity, only the proof for g_L (equation (5.3)) will be given. The derivations for g_R are similar.

Integrating the first term of (5.3) by parts we obtain

$$\underbrace{g_L(1)\,\phi(1)}_{\text{Term A}} - \underbrace{g_L(-1)\,\phi(-1)}_{\text{Term B}} - \underbrace{\int_{-1}^{1} g_L \nabla_r \phi \,\mathrm{d}r}_{\text{Term C}} = -\phi(-1). \tag{5.6}$$

If Term A and Term C are equal to 0 and $g_L(-1) = 1$, then (5.6) is valid.

Employing the left ESFR correction function, we have $g_L(-1) = 1$ and $g_L(1) = 0$ (Term A = 0). As for Term C, we have

$$\begin{aligned}&\int_{-1}^{1} g_L \nabla_r \phi \,\mathrm{d}r \\ &= \frac{(-1)^p}{2}\left[\int_{-1}^{1} \Psi_p \nabla_r \phi \,\mathrm{d}r - \frac{\eta_{p,\kappa}}{1+\eta_{p,\kappa}}\int_{-1}^{1} \Psi_{p-1} \nabla_r \phi \,\mathrm{d}r - \frac{1}{1+\eta_{p,\kappa}}\int_{-1}^{1} \Psi_{p+1} \nabla_r \phi \,\mathrm{d}r\right].\end{aligned} \tag{5.7}$$

$\nabla_r \phi$ is a polynomial of degree less than or equal to $p-1$ and hence can be decomposed in Legendre polynomials, $\phi = \sum_{i=0}^{p-1} \alpha_i \Psi_i$. Using Property A.2,

$$\int_{-1}^{1} g_L \nabla_r \phi \,\mathrm{d}r = \frac{(-1)^{p+1}\,\eta_{p,\kappa}\alpha_{p-1}}{(1+\eta_{p,\kappa})\,(2p-1)}, \tag{5.8}$$

which is equal to 0 if $\eta_{p,\kappa} = 0$ and hence if $\kappa = 0$. ∎

Remark 5.2. With $\kappa = 0$, the FR formulation in (5.5) is equivalent to the DG formulation in (5.2). Therefore, for $\kappa = 0$, the left ESFR correction function (respectively, right) is denoted $g_{L,DG}$ (respectively, $g_{R,DG}$).

Remark 5.3. Huynh [11] did not employ ESFR correction functions; instead he formulated g_L such that $g_L(-1) = 1$ (1 condition) and $g_L(1) = 0$ (1 condition). To recover the DG formulation the remaining requirement was to enforce g_L to be orthogonal to $\mathbb{P}_{p-1}$ (polynomials of degree $p-1$; p conditions). He then extended the FR formulation by relaxing the condition on Term C such that into g_L is orthogonal to $\mathbb{P}_{p-2}$ and thus obtained a large class of methods (1 free parameter). Vincent, Castonguay, and Jameson reduced this class and defined the ESFR methods [19] (see Definitions B.1 and B.2) which ensured the stability for the advection problem. Therefore for ESFR methods with $\kappa \neq 0$, the FR formulation in (5.5) is not equivalent to the DG formulation in (5.2). However, it has been shown [23] that the ESFR methods can be cast into a filtered DG method in any dimension and element type as well as the correction procedure via reconstruction formulation in one dimension [22].

An analogy between the correction function and the lifting operator, r^e, is now presented. Equation (2.12) makes us aware that the lifting operator r^e, for an edge e, is defined on both Ω_{n-1} and Ω_n and is a polynomial of degree p on both Ω_{n-1} and Ω_n (see Figure 2). We define the space $\Omega_e = \bigcup_{i=n-1}^{n} \Omega_i$. Similar to the affine mapping defined in (2.3), we define the surjection

$$\begin{aligned}\mathcal{M}_e^{-1}\colon \quad \Omega_e &\to [-1,1] \\ x &\mapsto \frac{(2x-(x_{n-1}+x_n))}{h_{n-1}}\,\chi|_{\Omega_{n-1}}(x) + \frac{(2x-(x_n+x_{n+1}))}{h_n}\,\chi|_{\Omega_n}(x),\end{aligned} \tag{5.9}$$

where $\chi|_{\Omega_i}(x)$ is equal to 1 if $x \in \Omega_i$ or 0 if $x \notin \Omega_i$.

LEMMA 5.4. *The lifting operators, r^e and l^e, employed in the BR2, CDG, and CDG2 numerical fluxes are equivalent to the following formulas:*

(5.10)
$$r^e\left(\llbracket u\rrbracket\right)(x) = \frac{\llbracket u_e\rrbracket}{2}\left[-\frac{1}{J_{n-1}}\nabla_r g_{R,DG}\left(\mathcal{M}_e^{-1}(x)\right)\chi|_{\Omega_{n-1}} + \frac{1}{J_n}\nabla_r g_{L,DG}\left(\mathcal{M}_e^{-1}(x)\right)\chi|_{\Omega_n}\right],$$

(5.11)
$$l^e\left(\beta\llbracket u\rrbracket\right)(x) = -\beta\llbracket u_e\rrbracket\left[\frac{1}{J_{n-1}}\nabla_r g_{R,DG}\left(\mathcal{M}_e^{-1}(x)\right)\chi|_{\Omega_{n-1}} + \frac{1}{J_n}\nabla_r g_{L,DG}\left(\mathcal{M}_e^{-1}(x)\right)\chi|_{\Omega_n}\right],$$

where $\nabla_r g_{L,DG}$ (respectively, $\nabla_r g_{R,DG}$) is the derivative with r of the left ESFR (respectively, right ESFR) correction function for $\kappa = 0$.

Proof. The lifting operator r^e is a polynomial of degree p on each element forming Ω_e. Using the definition of the lifting operator in (2.12),

(5.12)
$$\begin{aligned}\int_\Omega r^e\left(\llbracket u\rrbracket\right)\phi\,\mathrm{d}x &= -\llbracket u_e\rrbracket\{\!\{\phi\}\!\}_e \\ &= -\frac{\llbracket u_e\rrbracket}{2}\left[\phi\left(\mathcal{M}_e^{-1}(x_n)\right)\big|_{\Omega_{n-1}} + \phi\left(\mathcal{M}_e^{-1}(x_n)\right)\big|_{\Omega_n}\right],\end{aligned}$$

where $\phi|_{\Omega_{n-1}}$ (respectively, $\phi|_{\Omega_n}$) is the test function on Ω_{n-1} (respectively, Ω_n).

Employing Lemma 5.1,

(5.13)
$$\begin{aligned}&\int_{\Omega_e} r^e\left(\llbracket u\rrbracket\right)\phi\,\mathrm{d}x \\ &\quad= -\frac{\llbracket u_e\rrbracket}{2}\left[\int_{-1}^{1}\nabla_r g_{R,DG}\,\phi|_{\Omega_{n-1}}\,\mathrm{d}r - \int_{-1}^{1}\nabla_r g_{L,DG}\,\phi|_{\Omega_n}\,\mathrm{d}r\right] \\ &\quad= -\frac{\llbracket u_e\rrbracket}{2}\left[\frac{1}{J_{n-1}}\int_{\Omega_{n-1}}\nabla_r g_{R,DG}\,\phi|_{\Omega_{n-1}}\,\mathrm{d}x - \frac{1}{J_n}\int_{\Omega_n}\nabla_r g_{L,DG}\,\phi|_{\Omega_n}\,\mathrm{d}x\right] \\ &\quad= -\frac{\llbracket u_e\rrbracket}{2}\int_{\Omega_e}\left(\frac{1}{J_{n-1}}\nabla_r g_{R,DG}\,\chi|_{\Omega_{n-1}} - \frac{1}{J_n}\nabla_r g_{L,DG}\,\chi|_{\Omega_n}\right)\phi\,\mathrm{d}x,\end{aligned}$$

where $\phi = \phi|_{\Omega_{n-1}}\chi|_{\Omega_{n-1}} + \phi|_{\Omega_n}\chi|_{\Omega_n}$.

We gather all the terms in the same integral and we factor out the test function ϕ,

(5.14)
$$\int_{\Omega_e}\left(r^e\left(\llbracket u\rrbracket\right) + \frac{\llbracket u_e\rrbracket}{2}\left(\frac{1}{J_{n-1}}\nabla_r g_{R,DG}\,\chi|_{\Omega_{n-1}} - \frac{1}{J_n}\nabla_r g_{L,DG}\,\chi|_{\Omega_n}\right)\right)\phi\,\mathrm{d}x = 0.$$

This relation is true for any test function ϕ on Ω_e, hence retrieving (5.10). The formula for l^e is obtained similarly. ∎

5.1. Equivalence bewteen the IP and BR2 approaches.

THEOREM 5.5. *The BR2 formulation is equivalent to the IP formulation, both defined in* (2.10)*, if and only if*

$$s = \frac{8J_{n-1}J_n}{(J_{n-1}+J_n)(p+1)^2}\tau. \tag{5.15}$$

Proof. The only difference between the IP and the BR2 formulation is the penalty term; $-\tau[\![u]\!]$ for the IP numerical fluxes and $s\{\!\{r^e([\![u]\!])\}\!\}$ for the BR2 numerical fluxes. Lemma 5.4 yields

$$\begin{aligned} s\{\!\{r^e([\![u]\!])\}\!\} &= \frac{s}{2}\left(r^e([\![u]\!])_{e,-} + r^e([\![u]\!])_{e,+}\right) \\ &= \frac{s[\![u]\!]}{4}\left(-\frac{1}{J_{n-1}}g_{R,DG}^{'}(1) + \frac{1}{J_n}g_{L,DG}^{'}(-1)\right). \end{aligned} \tag{5.16}$$

We use Theorem B.3 ($g_{R,DG}^{'}(1) = -g_{L,DG}^{'}(-1)$) and then employ Property A.1 of the Legendre polynomial, which yields $g_{L,DG}^{'}(-1) = -\frac{(p+1)^2}{2}$ and hence

$$s\{\!\{r^e([\![u]\!])\}\!\} = -\frac{s[\![u_e]\!](p+1)^2}{8}\left(\frac{1}{J_{n-1}}+\frac{1}{J_n}\right). \tag{5.17}$$

We finally have

$$\begin{aligned} & & q^*_{e,BR2} &= q^*_{e,IP} \\ &\iff & s\{\!\{r^e([\![u]\!])\}\!\} &= -\tau[\![u_e]\!] \\ &\iff & -\frac{s[\![u_e]\!](p+1)^2}{8}\left(\frac{1}{J_{n-1}}+\frac{1}{J_n}\right) &= -\tau[\![u_e]\!] \\ &\iff & s &= \frac{8J_{n-1}J_n}{(J_{n-1}+J_n)(p+1)^2}\tau. \end{aligned} \tag{5.18}$$

∎

THEOREM 5.6. *Employing the BR2 formulation for the diffusion equation with the ESFR schemes, s greater than s^* implies the energy stability, with*

$$s^* = \frac{2\min_{\kappa}\left(|\nabla_r g_L(1)| - \nabla_r g_L(-1)\right)}{(p+1)^2} \implies \sum_{e=1}^{N_e}\Theta_e \le 0 \implies \frac{\mathrm{d}}{\mathrm{d}t}\|U\|^2_{p,c} \le 0. \tag{5.19}$$

Proof. Combining Theorems 5.5 and 4.4, we show that the BR2 formulation is equivalent to the IP formulation, and then we use the criterion of stability found for the IP numerical fluxes. ∎

5.2. BR2 numerical results. We launch the same suite of test cases as for the IP case, discussed in section 4.3. Due to the equivalency between the IP and BR2 in one dimension, we indeed obtain the same results as in Table 2 multiplied by the adapted factor $f = \frac{1}{4\pi}(p+1)^2 N_K$. These BR2 results are presented in Table 3.

Remark 5.7. Similar to Remark 4.6, Brezzi et al. derived a coercivity condition for the Poisson equation with the DG method and the BR2 formulation [4]: $s > 2$ (i.e., number of faces of an element) ensures the coercivity. Therefore the result obtained in (5.19) yields a sharper bound than the coercivity condition.

TABLE 3
s^*_{theory} *compared to* $s^*_{numerical}$ *for the BR2 formulation with* $p = 2$ *and* $p = 3$ *for* 32 *elements.*

p	2					3				
s^*_{theory}	0.67	0.67	0.67	0.67	0.67	0.75	0.75	0.75	0.75	0.75
c \ κ	κ_{DG}	κ_{SD}	κ_{Hu}	κ_+	10^5	κ_{DG}	κ_{SD}	κ_{Hu}	κ_+	10^5
c_{DG}	0.67	0.67	0.67	0.67	0.67	0.75	0.75	0.75	0.75	0.75
c_{SD}	0.67	0.67	0.67	0.67	0.67	0.75	0.75	0.75	0.75	0.75
c_{HU}	0.66	0.66	0.66	0.66	0.66	0.75	0.75	0.75	0.75	0.75
c_+	0.65	0.65	0.65	0.65	0.65	0.75	0.75	0.75	0.75	0.75
10^5	0.23	0.23	0.23	0.23	0.23	0.38	0.38	0.38	0.38	0.38

5.3. CDG/CDG2 energy stability condition.

THEOREM 5.8. *When the CDG or the CDG*2 *numerical fluxes are employed for the diffusion equation with the ESFR approach, choosing* τ *and* γ *such that the following relations hold ensures the energy stability:*

$$\tau_e^* \leq \tau + \gamma \frac{(p+1)^2}{8} \left(\frac{(1+2\beta)^2}{J_{n-1}} + \frac{(1-2\beta)^2}{J_n} \right) \tag{5.20}$$

for the CDG approach (where τ_e^* *is defined in* (4.13)*) and*

$$\tau_{IP,e}^* \leq \tau + \gamma \frac{(p+1)^2}{8} \left(\frac{(1+2\beta)^2}{J_{n-1}} + \frac{(1-2\beta)^2}{J_n} \right) \tag{5.21}$$

*for the CDG*2 *approach (where* $\tau_{IP,e}^*$ *is defined in* (4.19)*).*

Proof. To compute the CDG/CDG2 numerical fluxes (2.10), we need to derive the term $L^e(u)$. We have the relations

$$[\![r^e \left([\![u_e]\!] \right)]\!] = \frac{[\![u_e]\!] (p+1)^2}{4} \left(-\frac{1}{J_{n-1}} + \frac{1}{J_n} \right), \tag{5.22a}$$

$$\{\!\{ l^e \left(\beta [\![u_e]\!] \right) \}\!\} = -\frac{\beta [\![u_e]\!] (p+1)^2}{4} \left(\frac{1}{J_{n-1}} - \frac{1}{J_n} \right), \tag{5.22b}$$

$$[\![l^e \left(\beta [\![u_e]\!] \right)]\!] = -\frac{\beta [\![u_e]\!] (p+1)^2}{2} \left(\frac{1}{J_{n-1}} + \frac{1}{J_n} \right). \tag{5.22c}$$

Finally we obtain, with the definition of L^e in (2.13) and with (5.17),

$$L^e (u) = -\frac{[\![u_e]\!] (p+1)^2}{8} \left(\frac{(1+2\beta)^2}{J_{n-1}} + \frac{(1-2\beta)^2}{J_n} \right). \tag{5.23}$$

The penalty term of the CDG and CDG2 formulation is $-\tau [\![u_e]\!] + \gamma L^e(u) = -\tau_\gamma [\![u_e]\!]$ with $\tau_\gamma = \tau + \gamma \frac{(p+1)^2}{8} (\frac{(1+2\beta)^2}{J_{n-1}} + \frac{(1-2\beta)^2}{J_n})$. Upon taking τ_γ instead of τ in the proof of section 4.1, we obtain the stability condition for the CDG approach with (4.13) and for the CDG2 with (4.19). ∎

TABLE 4
L_2-errors $p = 2$.

		$\tau_{IP,e}$							$1.5\tau_{IP,e}$						
c	κ	N_K=32	N_K=64	N_K=128	OOA			$\Delta t_{\max}$	N_K=32	$N_K = 64$	N_K=128	OOA			$\Delta t_{\max}$
c_{DG}	κ_{DG}	9.88e-05	1.23e-05	1.53e-06	-	3.01	3.00	3.00e-03	8.42e-05	1.05e-05	1.30e-06	-	3.00	3.02	3.00e-03
	κ_+	9.88e-05	1.23e-05	1.53e-06	-	3.01	3.00	3.00e-03	8.42e-05	1.05e-05	1.30e-06	-	3.00	3.02	3.00e-03
c_{SD}	κ_{DG}	9.35e-05	1.16e-05	1.45e-06	-	3.01	3.00	5.00e-03	9.12e-05	1.10e-05	1.43e-06	-	3.05	2.95	4.20e-03
	κ_+	9.35e-05	1.16e-05	1.45e-06	-	3.01	3.00	5.00e-03	9.12e-05	1.10e-05	1.43e-06	-	3.05	2.95	4.20e-03
c_{HU}	κ_{DG}	8.68e-05	1.08e-05	1.34e-06	-	3.01	3.00	7.00e-03	7.45e-05	8.99e-06	1.16e-06	-	3.05	2.95	4.20e-03
	κ_+	8.68e-05	1.08e-05	1.34e-06	-	3.01	3.00	7.00e-03	7.45e-05	8.99e-06	1.16e-06	-	3.05	2.95	4.20e-03
c_+	κ_{DG}	7.26e-05	9.31e-06	1.16e-06	-	2.96	3.01	7.50e-03	5.08e-05	6.07e-06	7.73e-07	-	3.07	2.97	4.20e-03
	κ_+	7.26e-05	9.31e-06	1.16e-06	-	2.96	3.01	7.50e-03	5.08e-05	6.07e-06	7.73e-07	-	3.07	2.97	4.20e-03

TABLE 5
L_2-errors $p = 3$.

		$\tau_{IP,e}$							$1.5\tau_{IP,e}$						
c	κ	N_K=32	N_K=64	N_K=128	OOA			$\Delta t_{\max}$	K=32	$K = 64$	K=128	OOA			$\Delta t_{\max}$
c_{DG}	κ_{DG}	1.05e-05	1.31e-06	1.63e-07	-	3.01	3.00	1.00e-03	1.58e-06	1.02e-07	6.39e-09	-	3.95	4.00	1.00e-03
	κ_+	1.05e-05	1.31e-06	1.63e-07	-	3.01	3.00	1.00e-03	1.58e-06	1.02e-07	6.39e-09	-	3.95	4.00	1.00e-03
c_{SD}	κ_{DG}	9.66e-06	1.21e-06	1.51e-07	-	3.00	3.00	1.80e-03	1.45e-06	9.06e-08	5.73e-09	-	4.00	3.98	1.20e-03
	κ_+	9.66e-06	1.21e-06	1.51e-07	-	3.00	3.00	1.80e-03	1.45e-06	9.06e-08	5.73e-09	-	4.00	3.98	1.20e-03
c_{HU}	κ_{DG}	8.59e-06	1.07e-06	1.34e-07	-	3.00	3.00	2.10e-03	1.25e-06	7.86e-08	4.96e-09	-	4.00	3.99	1.20e-03
	κ_+	8.59e-06	1.07e-06	1.34e-07	-	3.00	3.00	2.10e-03	1.25e-06	7.86e-08	4.96e-09	-	4.00	3.99	1.20e-03
c_+	κ_{DG}	5.44e-06	6.72e-07	8.35e-08	-	3.02	3.01	2.30e-03	9.56e-07	5.98e-08	3.77e-09	-	4.00	3.99	1.20e-03
	κ_+	5.44e-06	6.72e-07	8.35e-08	-	3.02	3.01	2.30e-03	9.56e-07	5.98e-08	3.77e-09	-	4.00	3.99	1.20e-03

6. L_2-errors and orders of accuracy. In this section, investigation on the accuracy and explicit time step limits of the ESFR schemes for the diffusion equation are presented. The following MATLAB code [15] provides the numerical results presented in this article. In particular, we compare the IP/BR2 formulation on a one-dimensional domain to the LDG approach ($\beta = \frac{1}{2}$) through a careful study of the impact of the parameters, τ and κ. The problem considered is the same as in section 4.3. We employ LGL nodes and the time step has been chosen such that it corresponds to $\Delta t_{\max}$. Time advancement was achieved through the RK54 method.

The L_2-error was computed using LGL quadrature with order $p + 4$ (which provides sufficient strenght),

(6.1)
$$L_2 - error = \sqrt{\sum_{n=1}^{N_K} \int_{x_n}^{x_{n+1}} (u_n - u)^2 \, \mathrm{d}x} = \sqrt{\sum_{n=1}^{N_K} \left(\hat{\mathbf{u}}_n^T - \hat{\mathbf{u}}_{exact}^T\right) \mathbf{W} \left(\hat{\mathbf{u}}_n - \hat{\mathbf{u}}_{exact}\right)},$$

where $\mathbf{W}$ is the quadrature matrix of size $N_p \times N_p$. The following results may be extensive but the authors prefer to provide the exact numbers, to help the research community to replicate the results. Both parameters c and κ are modified, ranging from c_{DG} to c_+ and for κ_{DG} and κ_+. For brevity, only the results of three meshes are provided: $N_K \in \{32, 64, 128\}$. We also provide the OOA which is calculated based on the adjacent mesh size, as well as the maximal time step for 32 elements. Maximal time steps were evaluated through an iterative approach while ensuring that the solution remains bounded at $t = 1$. The numerical simulations have been replicated for two values of τ: $\tau_{IP,e}$ provided in (4.19) and $1.5\tau_{IP,e}$ for both $p = 2$ and $p = 3$.

Tables 4 and 5 list the absolute L_2-errors for each grid, OOA, and the maximum time step, $\Delta t_{\max}$. The OOA is evaluated between 32/64 and 64/128 elements. Several important observations can be made from the tables. First, at even degree of polynomials for $c \geq c_{DG}$ and at both $\tau_{IP,e}$ and $1.5\tau_{IP,e}$ the OOA is $p + 1$. Second, at uneven degree of polynomials for all combinations of $c \geq c_{DG}$ and $\tau_{IP,e}$, one order of convergence is lost (similar results were observed for the LDG numerical fluxes [7]). This loss is recovered when τ is increased to $1.5\tau_{IP,e}$. Surprisingly, we observe that c_+ yields the least L_2-error. Further investigations have been conducted and the authors

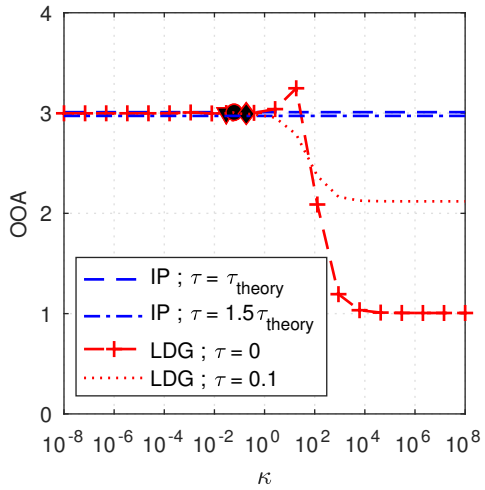

(a) Order of accuracy for $c = c_+$, $p = 2$.

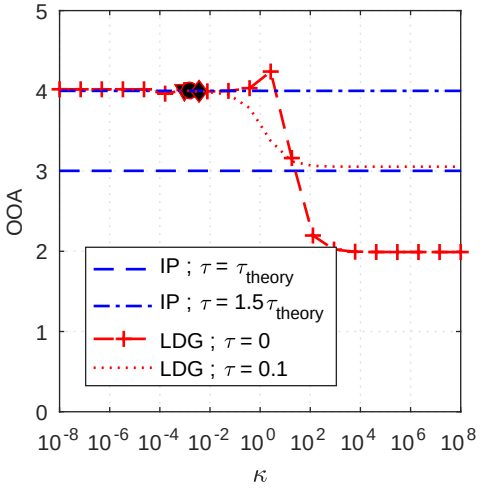

(b) Order of accuracy for $c = c_{DG}$, $p = 3$.

FIG. 4. *OOA along κ for different c and p, the lower triangle is for $\kappa = \kappa_{SD}$, the circle is for $\kappa = \kappa_{HU}$, and the diamond for $\kappa = \kappa_+$; using log scale the DG case couldn't be represented.*

have observed that for $c \geq c_+$, the L_2-errors resume increasing. As expected, κ has no influence. For the case c_{DG}, we observe that τ has an influence on the L_2-error but not on $\Delta t_{\max}$. After comparison with the work of Castonguay [6], we observe that the IP/BR2 numerical fluxes offer a higher time step with the same OOA as the LDG formulation.

We provide a comparison of the OOA between the IP and the LDG numerical fluxes. Orders are evaluated for κ in the range $[10^{-8}, 10^{8}]$ and two values of τ at $\tau_{IP,e}$ and $1.5\tau_{IP,e}$. The OOA is calculated between the two meshes: 64 and 128 elements. For brevity, only the cases $c = c_+$; $p = 2$ and $c = c_{DG}$; $p = 3$ are presented in Figure 4. Similar trends are observed for other values of c and for higher p. Several observations can be drawn from Figure 4. First, at even orders and for both values

of τ, the IP/BR2 numerical fluxes maintain a $p+1$ order. This is unlike LDG, where the orders are lost for $\kappa > \kappa_+$ for any τ. Second, for uneven orders (Figure 4(b)), the IP/BR2 numerical fluxes lose an order for $\tau_{IP,e}$ but recover the lost order when τ is increased. Numerical simulations have demonstrated that $\tau = 1.1\tau_{IP,e}$ is sufficient to provide a constant expected value of OOA for any p; however, too large a value of τ diminishes $\Delta t_{\max}$, as seen in Tables 4 and 5.

7. Conclusion. This article provided a theoretical proof of energy stability for the diffusion case using the IP numerical fluxes. This proof was then extended to the BR2/CDG and CDG2 numerical fluxes. For both of these numerical fluxes, the problem does not depend on κ. Numerical simulations have shown that pairing c close to c_+ with τ slightly greater than τ_{theory} provides both a high time step and a correct OOA. The proof can been extended to quadrilaterals and hexahedra with Cartesian grids, as was done by Sheshadri and Jameson [17] for the LDG scheme. Non-Cartesian grids yield a nonconstant Jacobian which leads to arduous derivations. However further investigations will be conducted in higher dimensions for triangular and tetrahedra grids.

Appendix A. Properties of Legendre polynomials. Throughout this work, we use ESFR correction functions, defined by Legendre polynomials of degree p: Ψ_p. These polynomials satisfy many properties easily found in any basic mathematical book. However, we will mention those used in this article.

Property A.1. Using Bonnet recurrence formula, we can show by induction that

$$\forall p \in \mathbb{N}, \Psi_p^{'}(1) = \frac{p(p+1)}{2} \text{ and } \Psi_p^{'}(-1) = (-1)^{p+1}\frac{p(p+1)}{2}. \tag{A.1}$$

Property A.2.

$$\int_{-1}^{1} \Psi_i \Psi_j \mathrm{d}r = \frac{2}{2i+1}\delta_{ij}, \text{where } \delta_{ij} \text{is the Kronecker delta.} \tag{A.2}$$

Property A.3. It can be shown, using a generating function,

$$\Psi_{p+1}^{'} - \Psi_{p-1}^{'} = (2p+1)\Psi_p. \tag{A.3}$$

Appendix B. ESFR correction functions. With these properties, we obtain an interesting theorem for the ESFR correction functions.

Definition B.1. *A left-ESFR correction function, g_L is, analytically, equal to*

$$g_L = \frac{(-1)^p}{2}\left[\Psi_p - \left(\frac{\eta_{p,\kappa}\Psi_{p-1} + \Psi_{p+1}}{1+\eta_{p,\kappa}}\right)\right], \tag{B.1}$$

where $\eta_{p,\kappa} = \frac{\kappa(2p+1)(a_p p!)^2}{2}$ *and* $a_p = \frac{(2p)!}{2^p(p!)^2}$.

Definition B.2. *A right-ESFR correction function, g_R is, analytically, equal to*

$$g_R = \frac{1}{2}\left[\Psi_p + \left(\frac{\eta_{p,\kappa}\Psi_{p-1} + \Psi_{p+1}}{1+\eta_{p,\kappa}}\right)\right]. \tag{B.2}$$

Theorem B.3. *Let g_L be a left-ESFR correction function and g_R be a right-ESFR correction function. Then*

$$g_L^{'}(r) = -g_R^{'}(-r). \tag{B.3}$$

Proof. This theorem is trivial if we consider the symmetry of the correction functions [19, equation (2.14)], $g_L(r) = g_R(-r)$. ∎

REFERENCES

[1] D. N. Arnold, *An interior penalty finite element method with discontinuous elements*, SIAM J. Numer. Anal., 19 (1982), pp. 742–760, https://doi.org/10.1137/0719052.

[2] F. Bassi and S. Rebay, *A high order discontinuous Galerkin method for compressible turbulent flows*, in Discontinuous Galerkin Methods, Lect. Notes Comput. Sci. Eng. 11, Springer, Berlin, 2000, pp. 77–88, https://doi.org/10.1007/978-3-642-59721-3_4.

[3] S. Brdar, A. Dedner, and R. Kölfkorn, *Compact and stable discontinuous Galerkin methods for convection-diffusion problems*, SIAM J. Sci. Comput., 34 (2012), pp. A263–A282, https://doi.org/10.1137/100817528.

[4] F. Brezzi, G. Manzini, D. Marini, P. Pietra, and A. Russo, *Discontinuous Galerkin approximations for elliptic problems*, Numer. Methods Partial Differential Equations, 16 (2000), pp. 365–378, https://doi.org/10.1002/1098-2426(200007)16:4⟨365::AID-NUM2⟩3.0.CO;2-Y.

[5] M. H. Carpenter and C. A. Kennedy, *Fourth-Order 2N-Storage Runge-Kutta Schemes*, Technical report, NASA, 1994, https://ntrs.nasa.gov/search.jsp?R=19940028444.

[6] P. Castonguay, *High-Order Energy Stable Flux Reconstruction Schemes for Fluid Flow Simulations on Unstructured Grids*, Ph.D. thesis, Stanford University, 2012, https://purl.stanford.edu/xf028gj8605.

[7] P. Castonguay, D. Williams, P. Vincent, and A. Jameson, *Energy stable flux reconstruction schemes for advection-diffusion problems*, Comput. Methods Appl. Mech. Engrg., 267 (2013), pp. 400–417, https://doi.org/10.1016/j.cma.2013.08.012.

[8] B. Cockburn and C.-W. Shu, *The local discontinuous Galerkin method for time-dependent convection-diffusion systems*, SIAM J. Numer. Anal., 35 (1998), pp. 2440–2463, https://doi.org/10.1137/S0036142997316712.

[9] H. T. Huynh, *A Flux Reconstruction Approach to High-Order Schemes Including Discontinuous Galerkin Methods*, American Institute of Aeronautics and Astronautics, 2007, https://doi.org/10.2514/6.2007-4079.

[10] H. T. Huynh, *A Reconstruction Approach to High-Order Schemes Including Discontinuous Galerkin for Diffusion*, American Institute of Aeronautics and Astronautics, 2009, https://doi.org/10.2514/6.2009-403.

[11] H. T. Huynh, *High-Order Methods Including Discontinuous Galerkin by Reconstructions on Triangular Meshes*, American Institute of Aeronautics and Astronautics, 2011, https://doi.org/10.2514/6.2011-44.

[12] J. S. Hesthaven and T. Warburton, *Nodal Discontinuous Galerkin methods Algorithms, Analysis and Applications*, Texts in Appl. Math. 54, Springer, New York, 2008.

[13] Y. Liu, M. Vinokur, and Z. Wang, *Spectral difference method for unstructured grids* I: *Basic formulation*, J. Comput. Phys., 216 (2006), pp. 780–801, https://doi.org/10.1016/j.jcp.2006.01.024.

[14] J. Peraire and P.-O. Persson, *The compact discontinuous Galerkin (CDG) method for elliptic problems*, SIAM J. Sci. Comput., 30 (2008), pp. 1806–1824, https://doi.org/10.1137/070685518.

[15] S. Quaegebeur, *1D_FRcode_Compact_Schemes*, https://github.com/sivanadarajah/1D_FRcode_compact_schemes.

[16] K. Shahbazi, *An explicit expression for the penalty parameter of the interior penalty method*, J. Comput. Phys., 205 (2005), pp. 401–407, https://doi.org/10.1016/j.jcp.2004.11.017.

[17] A. Sheshadri and A. Jameson, *An analysis of stability of the flux reconstruction formulation on quadrilateral elements for the linear advection–diffusion equation*, J. Sci. Comput., 74 (2018), pp. 1757–1785, https://doi.org/10.1007/s10915-017-0513-9.

[18] P. E. Vincent, P. Castonguay, and A. Jameson, *Insights from von Neumann analysis of high-order flux reconstruction schemes*, J. Comput. Phys., 230 (2011), pp. 8134–8154, https://doi.org/10.1016/j.jcp.2011.07.013.

[19] P. E. Vincent, P. Castonguay, and A. Jameson, *A new class of high-order energy stable flux reconstruction schemes*, J. Sci. Comput., 47 (2011), pp. 50–72, https://doi.org/10.1007/s10915-010-9420-z.

[20] W. H. Reed and T. R. Hill, *Triangular Mesh Methods for the Neutron Transport Equation*, Los Alamos Scientific Laboratory, Los Alamos, NM, 1973.

[21] Z. J. Wang, H. Gao, and T. Haga, *A unifying discontinuous formulation for hybrid meshes*, in Adaptive High-Order Methods in Computational Fluid Dynamics, Adv. Comput. Fluid Dyn. 2, World Scientific, River Edge, NJ, 2011, pp. 423–453, https://doi.org/10.1142/9789814313193_0015.

[22] M. Yu and Z. J. Wang, *On the connection between the correction and weighting functions in the correction procedure via reconstruction method*, J. Sci. Comput., 54 (2013), pp. 227–244, https://doi.org/10.1007/s10915-012-9618-3.

[23] P. Zwanenburg and S. Nadarajah, *Equivalence between the energy stable flux reconstruction and filtered discontinuous Galerkin schemes*, J. Comput. Phys., 306 (2016), pp. 343–369, https://doi.org/10.1016/j.jcp.2015.11.036.